The effect of coating defect distribution on buried steel pipelines on the effectiveness of cathodic protection

Über die Auswirkung der Verteilung von Umhüllungsfehlstellen auf erdverlegten Rohrleitungen auf die Wirksamkeit des kathodischen Korrosionsschutzes

M. Büchler, S. Collet and U. Angst*

SGK Swiss Society for Corrosion Protection
Technoparkstr. 1, CH-8005 Zürich,
markus.buechler@sgk.ch

*ETH Zürich, Institute for Building Materials
CH-8093 Zürich
ueli.angst@ifb.baug.ethz.ch

Abstract

In cathodic protection only limited attention is paid to the effect of lateral coating defect distribution as well as the current distribution within an individual coating defect. Nevertheless all measurement techniques inherently assume distant coating defects and a homogeneous current distribution within them. The effects associated with coating defect distance as well as heterogeneous current distribution are addressed by means of experiments and numerical simulation. The results are compared to literature data. The consequences of these effects on the durability of structures as well as the measurement techniques are discussed.

Zusammenfassung

Im kathodischen Korrosionsschutz wird der lateralen Verteilung von Umhüllungsfehlstellen sowie der Verteilung der Stromdichte innerhalb von Fehlstellen nur wenig Aufmerksamkeit geschenkt. Insbesondere nehmen alle Messverfahren eine grosse Distanz zwischen einzelnen Fehlstellen sowie eine homogene Stromverteilung innerhalb der Fehlstellen an. Die damit zusammenhängenden Effekte werden mit Hilfe von Experimenten sowie numerischer Simulation untersucht. Die Resultate werden mit Literaturdaten verglichen. Die Auswirkungen dieser Effekte auf die Dauerhaftigkeit von Strukturen sowie die Messmethoden werden diskutiert.

1. Introduction

Cathodic protection (CP) has been systematically applied since 1928 when Robert Kuhn proposed this technique to mitigate corrosion on pipelines [1]. He proposed an on-potential (E_{on}) criterion of -0.85 V_{CSE}. Also, he identified the galvanic corrosion among differently aerated coating defects as the reason for the high corrosion rates. Furthermore, he observed that applying a sufficiently negative on-potential ensures the compensation of these galvanic couples and a strong limitation of the corrosion process. Kasahara, Sato and Adachi [2] as well as Thompson and Barlo [3] demonstrated that even current densities as small as 1 mA/m^2 would result in an important increase of the pH well above 9 under limited mass transport conditions at the steel surface in case of cathodic protection. At these pH values the formation of a passive film is expected based on the thermodynamic considerations of Pourbaix [4]. Thus, for well bedded coating defects allowing for concentration polarization and an increase of pH, corrosion protection is achieved through passivation, as discussed in detail in [5] and [6]. The good success of Kuhn's on-potential criterion can hence readily be explained: The small current density required for the increase of the pH at the steel surface required for passivation in the range of 1 mA/m^2 will not cause any relevant ohmic drop. After the formation of the passive film, the current densities and hence the ohmic drops will significantly increase as discussed in [7] as a result of the strongly deceased anodic dissolution current on the passive surface. Thus, the current density is controlled by the diffusion limited oxygen reduction current. In well aerated soils this can be in the range of 0.1 to 1 A/m^2 [8]. In the case of a heterogeneous current distribution a non-uniform increase of the pH at the steel surface is achieved. This can result in partial passivation and associated corrosion problems.

The problems of heterogeneous passivation were described in detail by Evans in 1923 for the corrosion of steel in heterogeneous aeration [9]. In order to illustrate his concept and the associated problems with partial passivation, the relevant effects are discussed by means of the Evans droplet test:

A piece of steel with a water droplet on top will develop within a few minutes a localized corrosion process based on the reduction of oxygen according to equation (1) and the oxidation of iron according to equation (2).

$$O_2 + 2H_2O + 4e^- \rightarrow 4OH^- \quad (1)$$

$$2Fe \rightarrow 2Fe^{2+} + 4e^- \quad (2)$$

The heterogeneous aeration due to the different diffusion distances for oxygen causes an increase of the pH at the edges of the droplet while oxygen depletion in the center will result in increased corrosion. This mechanism originally reported by Evans was summarized by Pourbaix [4] in 1974 as follows:

"When a piece of iron is immersed in a practically neutral non-buffered solution, which is aerated in one region (edges of the droplet) and not aerated in another (center of the droplet), it is noticed that this differential aeration produces an increase in the corrosion rate in the non-aerated regions, and a decrease in the corrosion rate in the aerated regions, with a flow of electric current between these regions. On account of the increase of the pH due to the reduction of oxygen, the aerated regions will be passivated and the non-aerated regions will not be passivated."

Based on the above discussion it can readily be argued that this very configuration could occur within an individual coating defect of a buried pipeline before the application of cathodic protection. Hence the presence of homogeneous current distribution may not necessarily be assumed. Therefore, the complete passivation within the coating defect cannot be expected under all circumstances. Additionally, the current entering the coating defect will be non-uniformly distributed across the defect area, i.e. the current density will be higher towards the edges of the coating defect, while the central part will receive lower protection current densities.

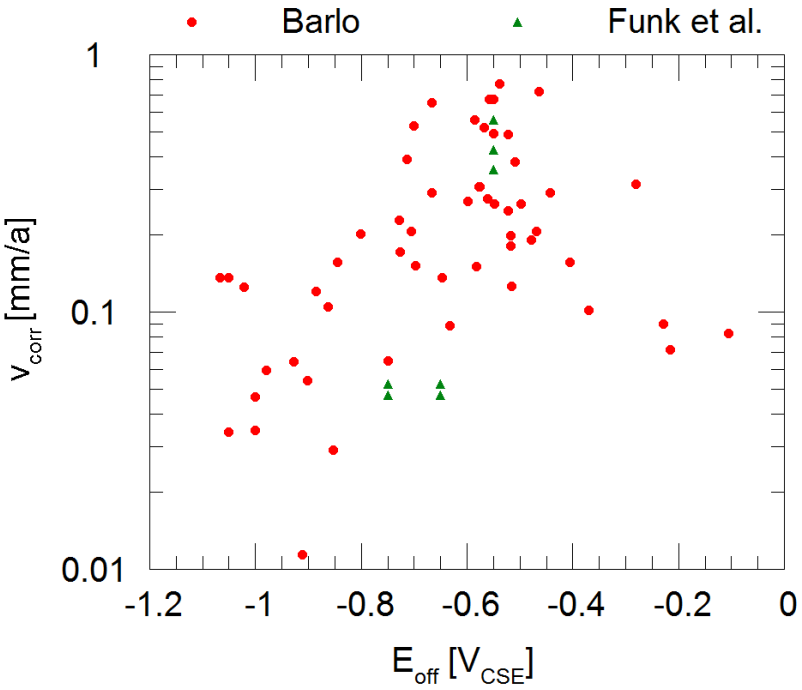

Figure 1: **Maximum local corrosion rate on coupons with a surface of 5 m^2 reported by Barlo [10] and 25 cm^2 reported by Funk et al [8].**

The effect of partial passivation and increased local corrosion rates is, therefore, expected to result in non-uniform corrosion rates as reported by Barlo [10] (Figure 1). His field tests on non-coated pipes with a length of 3 m and a surface of about 5 m^2 confirmed significantly increased local corrosion rates. The local corrosion rate is more pronounced at instant-off potentials in the range of -0.6 V_{CSE}. But even at instant off potentials as negative as -1.1 V_{CSE} local corrosion rates of 0.1 mm/year were observed. Similar results are reported in field tests by Funk et al [8] for coupons of 25 cm^2 (Figure 1). The increased local corrosion rates were attributed to the formation of galvanic elements within the coupon. This is in line with a partial passivation of the steel surface. It is relevant to note that the protection criteria of -0.75 and -0.65 V_{CSE} in ISO 15589-1 in conjunction with a maximum corrosion rate of 0.01 mm/year are based on the data of Funk et al [8], that specifically report corrosion rates as high as 0.05 mm/year. These results confirm the relevance of heterogeneous current distribution on the local corrosion rate. They also raise the question regarding the applicability of the protection criteria in in ISO 15589-1 in conjunction with the maximum corrosion rate of 0.01 mm/year. All of the presented data in Figure 1 exhibit higher corrosion rates even when the protection criteria were met for the instant off potential on the coupon.

Increased local corrosion rates can readily cause a severe durability issue on pipelines. Therefore, the consequences resulting from heterogeneous current distribution on the expected

corrosion behavior and the associated measurement techniques as well as the corresponding geometrical configurations will be discussed based on experiments and numerical simulation.

2. Experimental

2.1. Artificial soils

All solutions were prepared from reagent grade chemicals and de-ionized water. For the simulation of the behavior in soil, coupons were exposed to artificial soil solution in quartz sand with grain sizes ranging from 0.3 to 0.9 mm. The composition of the electrolyte is given in Table 1.

Table 1: Composition of the artificial soil solution

$NaHCO_3$	2.5 mmol/l
$NaSO_4*10H_2O$	5 mmol/l
NaCl	5 mmol/l

Soil aeration is a key factor for the corrosion process. Hence, well aerated conditions were simulated by mixing artificial soil solution with dry sand in a ratio yielding saturation of approx. a quarter of the pore volume in the sand.

2.2. Coupons

Different coupons were manufactured from both, mild steel rods with a diameter of 29 mm or stainless steel (1.4301) rods with a diameter of 22 mm. They were cast into an epoxy cylinder with a diameter of 40 mm (Figure 2). In the case of the coupons made of stainless steel in the center a mild steel electrode with 2 mm diameter was installed (see Figure 3); the inner and the outer steel electrodes were electrically isolated from each other by means of an epoxy resin to allow for individual current measurement through external short-circuiting according to Figure 3. The coupons were polished with grit 400 and rinsed with distilled water and directly placed in the test setup. Most of the experiments were made inside 2 liter cylindrical plastic boxes (Figure 2) with a mesh anode against the inside walls. Rectangular plastic boxes with a dimension of 60x40x20 cm were used to measure the influence of the distance between different coating defects.

2.3. Electrochemical testing

In case of the experiments in 2 liter cylindrical plastic containers large surface mixed metal oxide covered titanium mesh (MMO) anodes were placed on the walls of the containers. All potential readings were taken against a reference electrode placed on the soil surface at a position considered as “neutral earth”, i.e. outside of local gradients. Currents were measured by means of shunt resistors of 10 to 1000 Ω and a micro voltmeter that was placed in the electrical connection between the two electrodes electrically connected in the different test setups simulating galvanic corrosion.

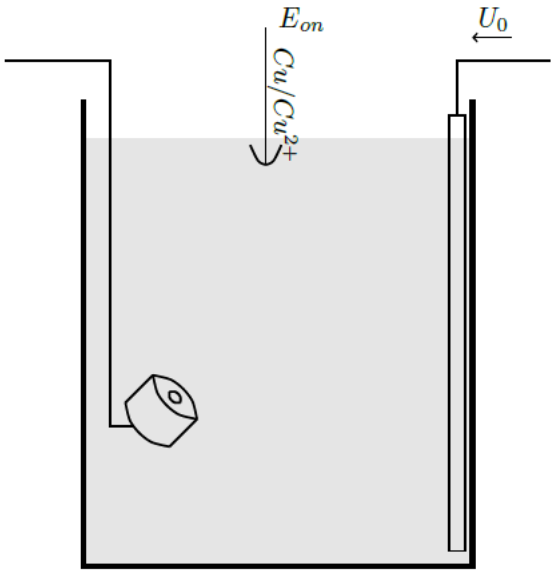

Figure 2: **Experimental setup, 2 liter cylindrical plastic box**

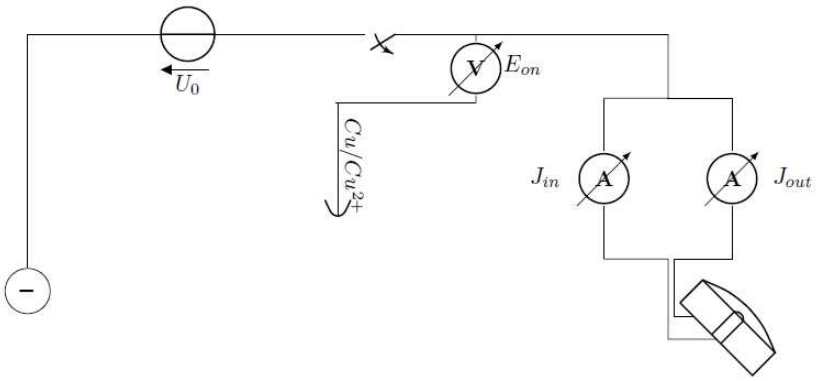

Figure 3: **Electrical scheme of the setup.**

Three different types of experiments were carried out to address the following issues. Throughout all tests, the temperature was ca. 20-22 ℃.

a) Influence of the distance between the electrodes

A 22 mm diameter stainless steel coupon and a 2 mm diameter mild steel coupon were buried in artificial soil and electrically connected to form a galvanic element, both at the same distance from the anode. Both coupons were polished prior to every experiment. Once embedded in the soil, cathodic polarization was applied by means of a potentiodynamic scan, controlled vs. the reference electrode positioned on neutral earth (no IR drop compensation). The applied potentials were between -0.5 V_{CSE} (starting potential) and -1.5 V_{CSE} (on-potentials). The scan rate was 1 mV/s = 0.36 V/h.

The influence of the geometry on corrosion currents was obtained by varying the distance between the coupons: L_{cd} was 25 cm, 1 cm, and 0 cm, where the last case is the one with the mild steel electrode being positioned in the very center of the stainless steel electrode.

b) Effect of potential scan rate

A galvanic element was simulated with a 2 mm mild steel electrode in the center of a stainless steel coupon with a diameter of 22 mm. This represents a typical pitting configuration. This freshly polished coupon was buried in artificial soil and cathodic polarization was applied by means of a potentiodynamic scan, controlled vs. the reference electrode positioned on neutral earth (no IR drop compensation). The applied potentials were between -0.5 V_{CSE} (starting potential) and -2.2 V_{CSE}. Different scan rates were studied, namely 0.1 V/h, 1 V/h and 10 V/h.

c) Long-term effect of cathodic protection

The aim was to investigate the behavior of an actively corroding electrode (2 mm mild steel) in the center of a passive electrode (29 mm mild steel) under long-term application of a cathodic protection current. Initially, upon embedding the combined coupon in soil, a constant current of 0.5 mA was applied between the two electrodes during 1 hour. The small electrode in the center was the anode, while the outer electrode acted as cathode. Subsequently, the two pre-polarized electrodes were electrically connected and let without any externally impressed current during 10 hours, which was sufficient to obtain a stable galvanic corrosion process.

Based on these initial conditions three different experiments were carried out (each on a new setup, freshly preconditioned as described above). In all cases, the current leaving/entering the mild steel electrode in the center was monitored over time.

- Long-term experiment 1: A constant on-potential of -1.2 V_{CSE} was applied.
- Long-term experiment 2: No externally applied polarization, but the combined coupon was embedded in sand mixed with $Ca(OH)_2$ powder in order to obtain a well buffered alkaline soil.

2.4. Numerical modelling

The numerical modelling was based on the concepts given in [7, 11-13] that assume a homogeneous current distribution. The heterogeneity was incorporated by considering two individual coating defects with homogeneous current distribution each, whose distance was varied. For simplicity, the spread resistance of the anode with diameter d was calculated according to equation (3) [14] for a hemispherical electrode and a homogeneous soil resistivity ρ.

$$R = \frac{\rho}{\pi \cdot d} \tag{3}$$

The effect of pH change on local resistivity caused by cathodic currents as discussed in detail in [5] is taken into account based on the equations given in [15, 16].

3. Results and discussion

3.1. Introduction

The distance between two coating defects (L_{cd} ,distance between their central points) is a key parameter in the further discussion. In order to investigate the effect of L_{cd} as well as partial passivation on the corrosion protection, various distances between coating defects were tested in laboratory set-ups as well as with numerical modelling. The effect of L_{cd} on the on-potential required to obtain a change in polarity of the current on the anode was investigated. Furthermore, an extreme configuration of a small active steel electrode within a larger passive surface (L_{cd} = 0) was simulated by using a mild steel electrode (diameter 2 mm) in the center of a larger stainless steel electrode (diameter 22 mm). The conditions required for cathodic protection were analyzed in this configuration. Finally, the long term effects were analyzed in order to gain an understanding of the underlying mechanisms.

3.2. Effect of distance between individual coating defects

The results in Figure 4 show the behavior of two coating defects of mild steel and stainless steel in well aerated soil with resistivity of 800 Ωm. At L_{cd} = 25 cm cathodic currents already are obtained on the mild steel electrode at on-potentials as positive as -0.6 V_{CSE}. At this distance in these soil conditions any galvanic corrosion between the two coating defects is eliminated by an on-potential more negative than -0.6 V_{CSE} in the case of the scan rate of 1 mV/s. In the case of L_{cd} = 1cm, an on-potential as negative as -1 V_{CSE} is required in order to obtain cathodic currents. The worst case is given by the stainless steel coupon surrounding the mild steel electrode (L_{cd} = 0 cm), leading to anodic current even with an E_{on}= -1.5 V_{CSE}. This demonstrates the relevance of L_{cd} in the case of two individual coating defects with passive and active behavior. The on-potential values determined for current inversion for the various configurations are only valid for the given experimental setup. They cannot be taken as a valid criterion for cathodic protection on a real structure. The influence of the scan rate is discussed in detail in section 3.3.

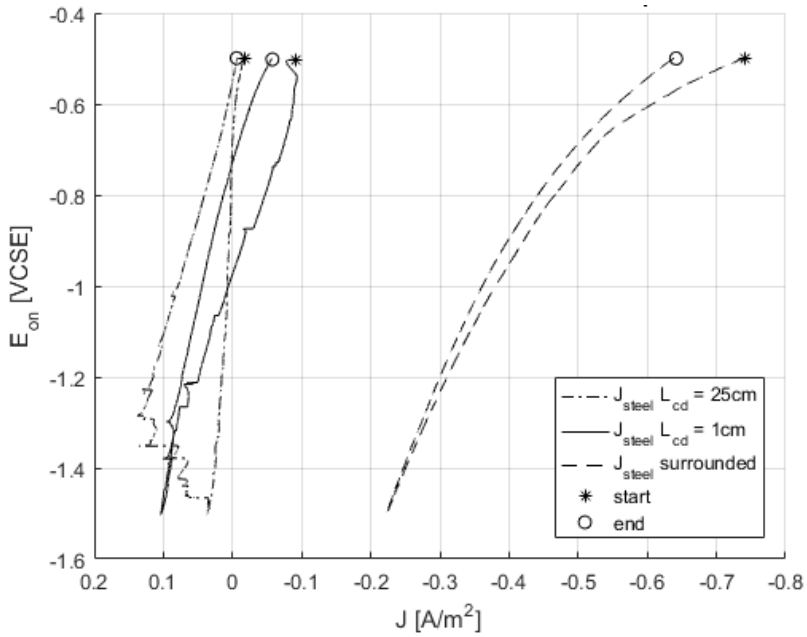

Figure 4: **Currents of a 2mm diameter mild steel coupon at several distances from a 22mm stainless steel coupon (L_{cd}). ρ = 800 Ωm, Scan rate = 1mV/s.**

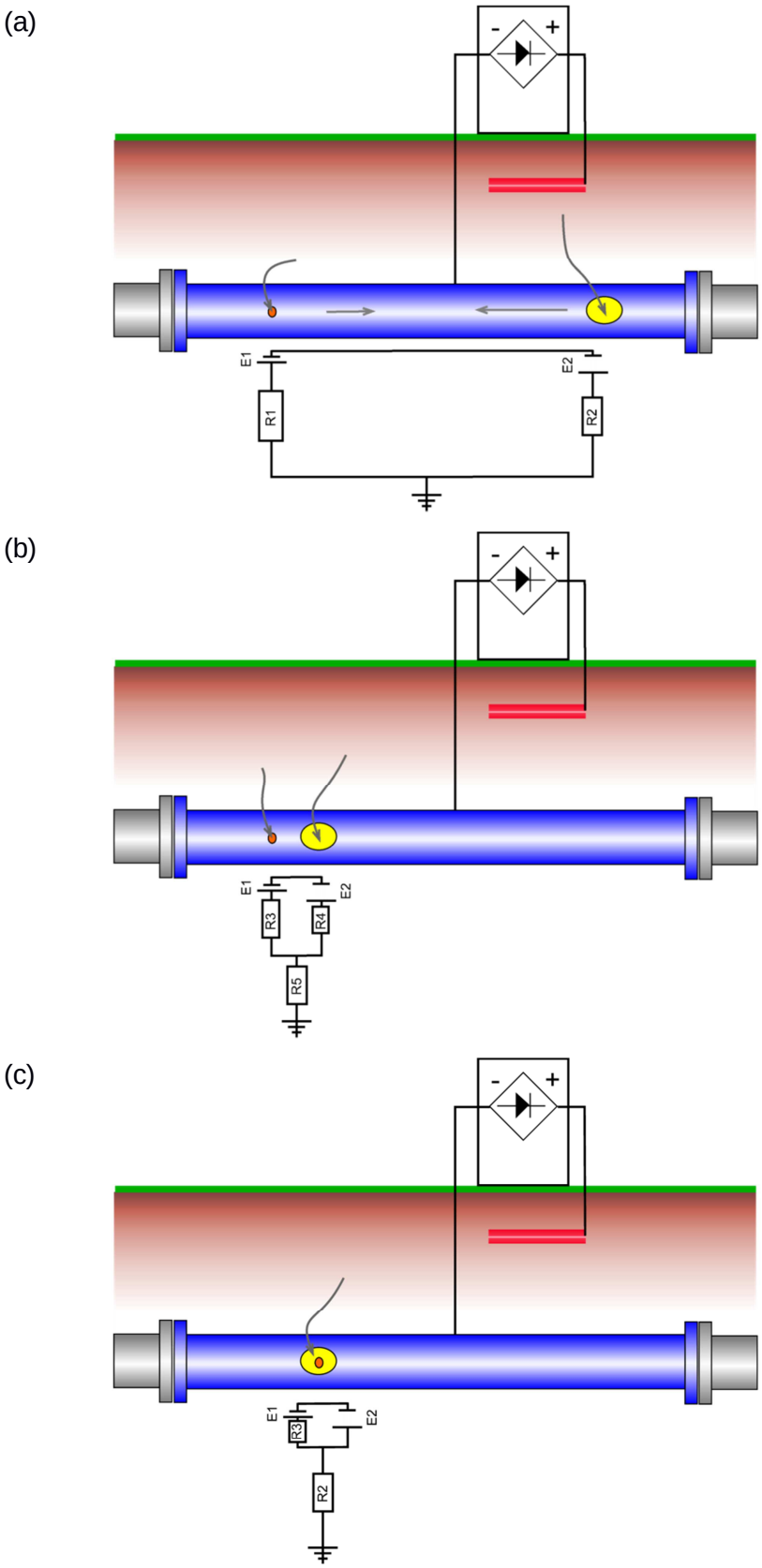

Figure 5: **Effect of L_{cd} on the corrosion behavior of a large well aerated coating defect (yellow) and a small coating defect (red). The cathodic currents are symbolized by the arrows: a) L_{cd} is large, the coating defects can be taken as two independent systems; b) L_{cd} is small, the coating defects influence each other; c) L_{cd} is zero, the small coating defect is inside the larger well aerated coating defect.**

The observed behavior can be explained based on the ohmic drop generated by the ionic current in the ground. In the case of a large L_{cd} the spread resistance is controlled independently by each individual coating defect according to equation (3) as illustrated in Figure 5a. Despite of different IR-free potentials (E1 and E2) of the individual coating defects a sufficiently negative on-potential assures a current to enter in each coating defect according to equation (4).

$$I = \frac{E_{IR-free} - E_{on}}{R} \tag{4}$$

In Figure 5a the different IR-free potentials are illustrated by means of the distance between the two schematic electrodes at E1 and E2. E1 symbolizes a more negative potential, while E2 with the larger distance between the two parallel lines in the schematic drawing symbolizes a more positive IR-free potential as expected on a passive electrode in a well aerated soil. E1 and E2 can be considered as the two half cells of the galvanic couple that would establish in absence of cathodic protection.

With decreasing L_{cd} the ohmic drops of each individual coating defect start to influence each other, as shown in Figure 5b. In this case the different IR-free potentials (E1 and E2) result in a galvanic current between the coating defects even with Eon more negative than -0.85 V_{CSE}. Since the ohmic drop over R5 is relevant, the current flow on the individual coating defects is no longer solely controlled by Eon against remote earth. As a consequence, more negative Eon values are required to overcome this galvanic element in the case of decreased L_{cd}.

If L_{cd} is zero as illustrated in Figure 5c, the galvanic current can only be overcome if the cathodic protection current polarizes E2 cathodic of E1. In correspondence with Figure 5a and ohms law the polarization of E2 more cathodic of -0.85 V_{CSE} will be required in order to assure a current to enter into both coating defects.

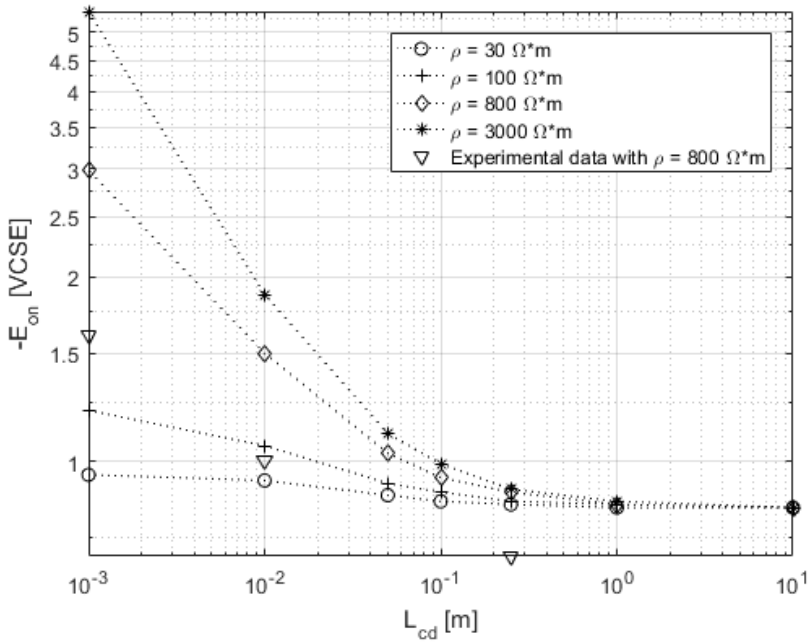

Figure 6: **Numerical approximation of Eon threshold values for current inversion in the small coupon with several distance and soil resistivity. L_{cd} of 10^{-3} represents the configuration in Figure 5c. Large coupon: diameter = 22mm; well aerated conditions (J_{ox} = 1 A/m^2). Small coupon: diameter = 2mm; anaerobic conditions (J_{ox} = 0 A/m^2).**

Based on the simplified numerical model the main controlling parameters of the system (coating defect sizes, aeration, soil resistivity, E_{on}, and L_{cd}) were applied to calculate the relevant parameters and compare them to the experimental data (Figure 6). The model assumed anaerobic conditions on the small coating defect (diffusion limited oxygen reduction current density (Jox = 0 A/m^2) and well aeration on the larger defect (Jox = 1 A/m^2). Based on the model the Eon measured against remote earth was calculated as a function of L_{cd} at which the anaerobic metal surface received cathodic current. Based on Figure 6 for large values of L_{cd} an Eon of -0.85 V_{CSE} was sufficient to ensure a cathodic current. With decreasing L_{cd} and increasing ρ the required Eon for changing the polarity of the current shifted to more negative values.

The experimental data show lower threshold values for current inversion than the ones calculated. It may be due to the non-anaerobic for the small coating defect in the experiment. Figure 7 shows the corresponding results for a larger size of the coating defect with a diameter of 100 mm. The increased coating defect surface clearly results in significantly more negative E_{on} values as negative as 20 V_{CSE} in order to achieve a cathodic current on all defect surfaces, demonstrating the relevance of the geometrical conditions. This is in line with the significantly increased corrosion rates reported for larger defect sizes as shown in Figure 1.

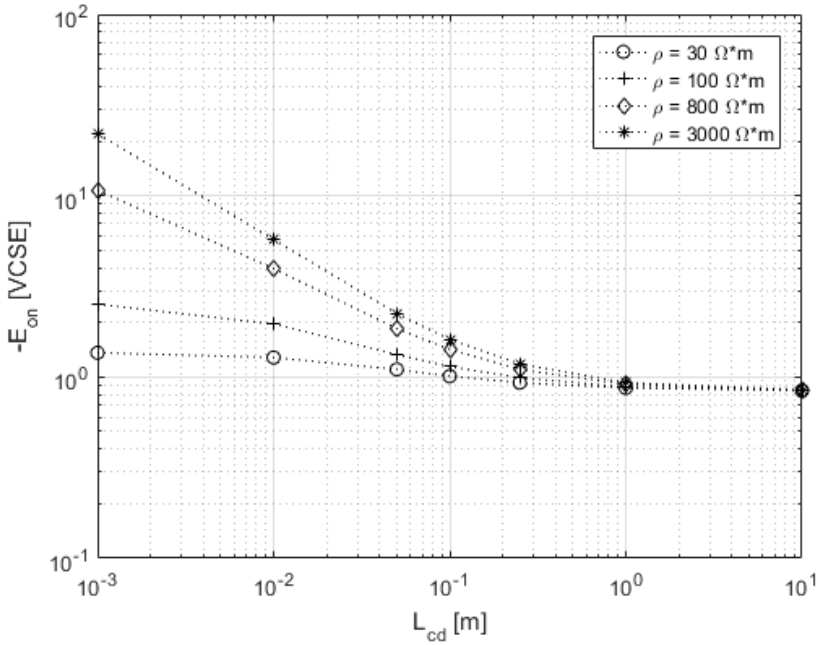

Figure 7: **Numerical approximation of E_{on} threshold values for current inversion in the small coupon with several distance and soil resistivity. L_{cd} of 10^{-3} represents the configuration in Figure 5c. Large defect: diameter = 100mm; well aerated conditions (J_{ox} = 1 A/m^2). Small coupon: diameter = 2mm; anaerobic conditions (J_{ox} = 0 A/m^2).**

Based on these results, the interpretation of the increased corrosion rates in the range of 0.05 mm/year by Funk et al. [8] as galvanic corrosion within the individual coating defect is fully in line with Figure 5c. As a consequence the results in Figure 1 can be readily explained by heterogeneous aeration, the generation of local galvanic elements and partial passivation of the steel surface.

3.3. Establishing protection on heterogeneous coating defects

The investigation of L_{cd} with respect to the corrosion behavior demonstrates a significantly increased corrosion risk for cathodically protected structures in well aerated soils with increased soil resistivity and in presence of large coating defects. Even meeting the appropriate protection criteria for the IR-free potential in ISO 15589-1 (e.g. -0.85 V_{CSE}) does not exclude relevant corrosion rates as clearly demonstrated in Figure 1. Protection can only be achieved at significantly more negative potential values. In the presence of large coating defects unrealistically negative Eon values may be required, as must be concluded based on the calculations in Figure 7. Hence the question arises with respect to the mechanism influencing the protection.

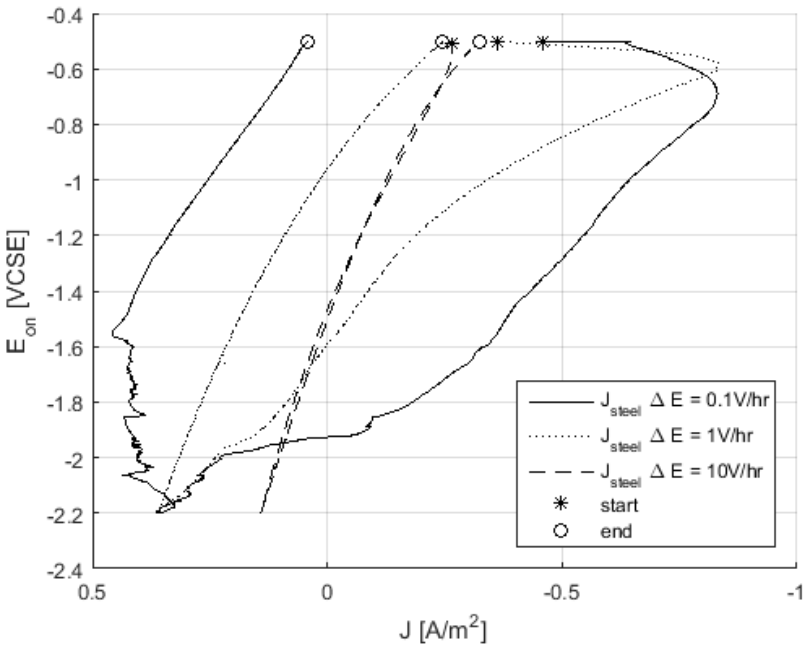

Figure 8: **Effect of the scan rate (ΔE) on corrosion behavior.Current of a 2mm diameter mild steel coupon surrounded by a 22mm stainless steel area (both electrodes short-circuited). CP potential increase between -0.5 and -2.2 VCSE with several scan rates. ρ = 600 Ωm, well aerated conditions (10 %vol)**

This was investigated based on 2 mm steel electrodes in the center of a 22 mm diameter stainless steel coupon that was subjected to potential cycling with different scan rates. The results are shown in Figure 8. Based on these results an important hysteresis of the current density of the 2 mm diameter steel electrode is observed for the slower scan rates of 0.1 and 1 V/hr. At these slow scan rates, the anodic current leaving the steel electrode initially increased markedly during the cathodic shift of the potential, which is attributed to the local acidification caused by the anodic current. With the further shift of Eon to more negative values the anodic current decreases and becomes cathodic in the case of all scan rates. Interestingly, the Eon required for inversion of the current direction is more negative in the case of the slow scan rates. Upon inversion of the scan direction, a relevant hysteresis is found for the two slower can rates. In the case of 0.1 V/h the current does not become anodic anymore when returning to the starting potential.

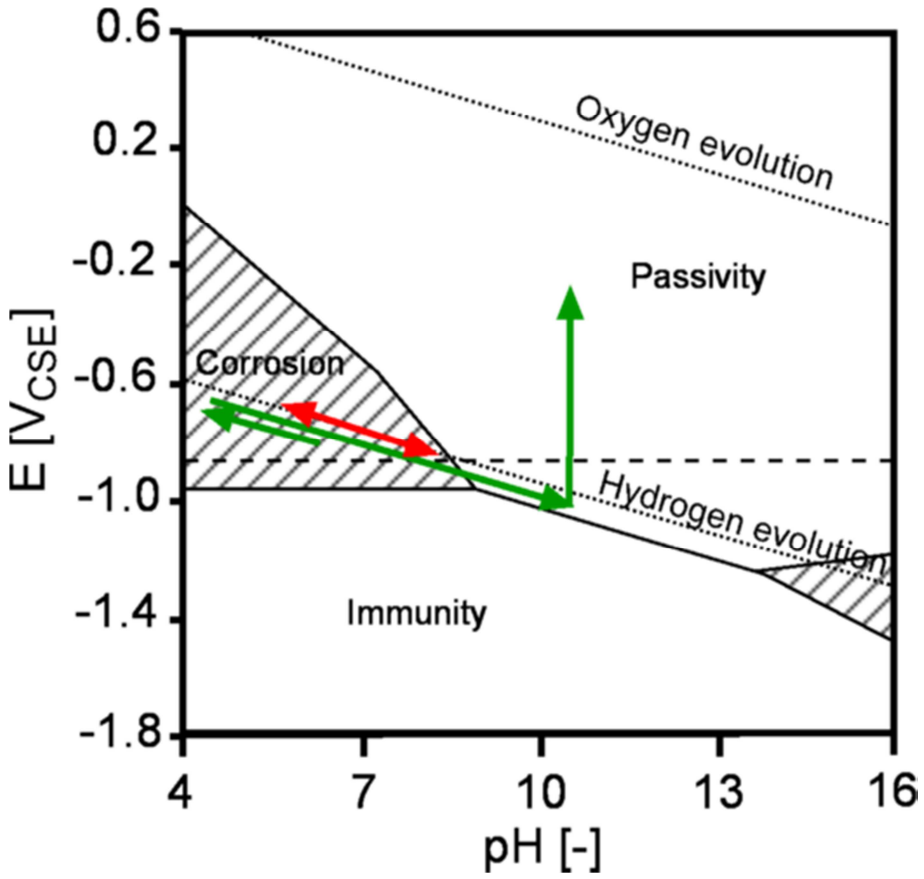

Figure 9: Effect of the scan rate on the corrosion behavior. Red: 10 V/h; Green: 0.1 V/h

The important time dependence clearly shows the relevance of slow processes taking place at the steel surface. As discussed in [5, 6], the accumulation of hydroxide ions and the associated increase of the pH at the steel surface is a critical factor in achieving cathodic protection of steel through passivation. The hypothesis is that the anodic currents result in a decrease of the pH at the steel electrode. As a consequence, the anodic charge passed during the initial stages results in a relevant acidification at the surface of the steel electrode. This is more pronounced in the case of slow scan rates as shown schematically for 0.1 V/h in Figure 9. The higher anodic charge causes a more significant acidification. As a consequence more negative on-potentials are required to compensate the galvanic element. In contrast, the higher cathodic charge also results in a stronger increase of the pH and the generation of the conditions for passive film formation. This increase in pH will be more pronounced in the case of slower scan rates due to the larger amount of cathodic charge passed. This results in cathodic currents at potentials as positive as -0.5 V_{CSE} similarly to the stainless steel electrode. In contrast, the higher scan rates do not allow for significantly changing the pH conditions at the surface of the steel electrode as illustrated in Figure 9. Under these conditions no passivation and hence no hysteresis is observed.

From these results it is inferred that the application of a short term strong cathodic polarization can result in passivation of the residual anodic sites.

3.4. Long-term effect of an alkaline environment

The increase of pH at the steel surface was demonstrated to be beneficial in the case of a cathodic polarization of the steel surface. This raises the question with respect to the effect of a

significantly increased pH in the environment as it can be expected under long term cathodic protection or in concrete. It could be argued that the increased pH in the vicinity of the steel electrode will result in the transport of hydroxides to the anodic site due to diffusion and migration. Over time a neutralization of the acid at the anode and an increase of the pH in the anodic site could be postulated.

This effect was investigated with a coupon consisting of a 2 mm diameter steel electrode that was placed in the center of a 29 mm diameter steel electrode (L_{cd} = 0). The center electrode was activated initially by an anodic current of 0.5 mA of 1 hour duration applied between the two electrodes.

Figure 10 shows the evolution of the current flowing through the 2 mm electrode after the pre-treatment. The experiment in sand with neutral soil solution in combination with a cathodic protection with an Eon of -1.2 V_{CSE} showed still relevant corrosion after 3 days with a rate of 5.8 mm/year at an IR-free potential of -0.68 V_{CSE}. However, passivation occurred after 5 days and the current density then remained cathodic until the end of the experiment with no relevant corrosion at an IR-free potential of -0.7 V_{CSE}.

Identical coupons with the same pretreatment buried in sand mixed with $Ca(OH)_2$ powder in order to obtain an alkaline buffered soil were investigated as well. Both electrodes were electrically connected, but without any external current applied. In this case after 9 days the polarity of the electrode changed.

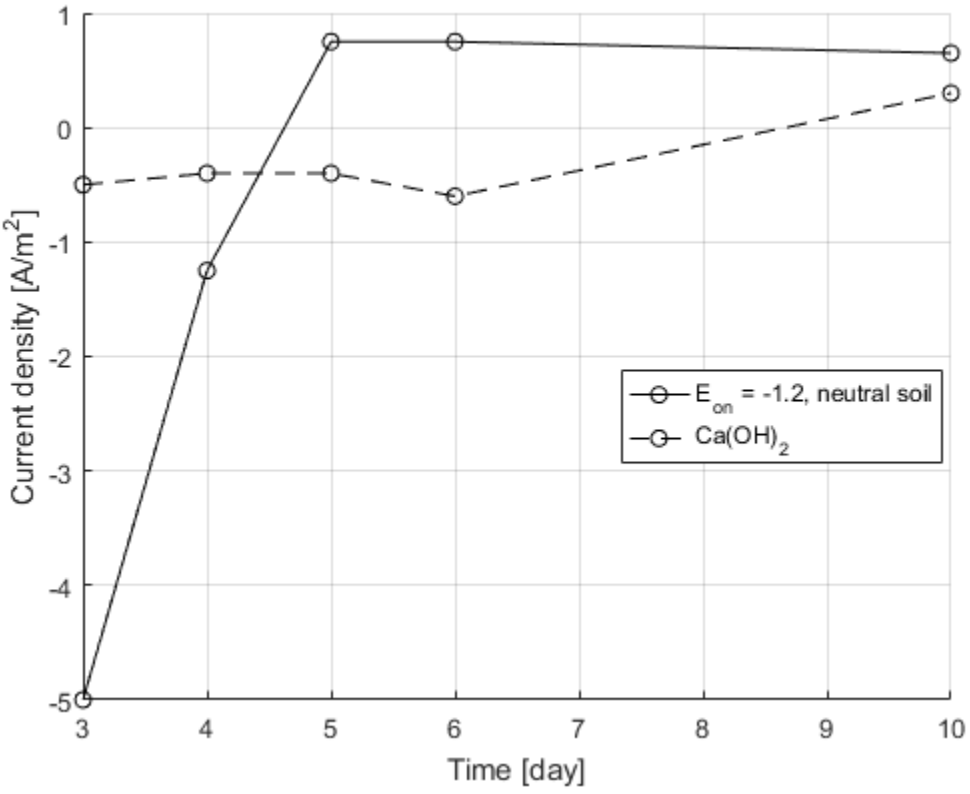

Figure 10: **Corrosion current over 10 days experiment with constant CP. Eon = -1.2 VCSE in neutral artificial soil, well aerated condition (10% vol.); No CP in basic buffered soil with pH = 12.5, well aerated condition (10% vol.)**

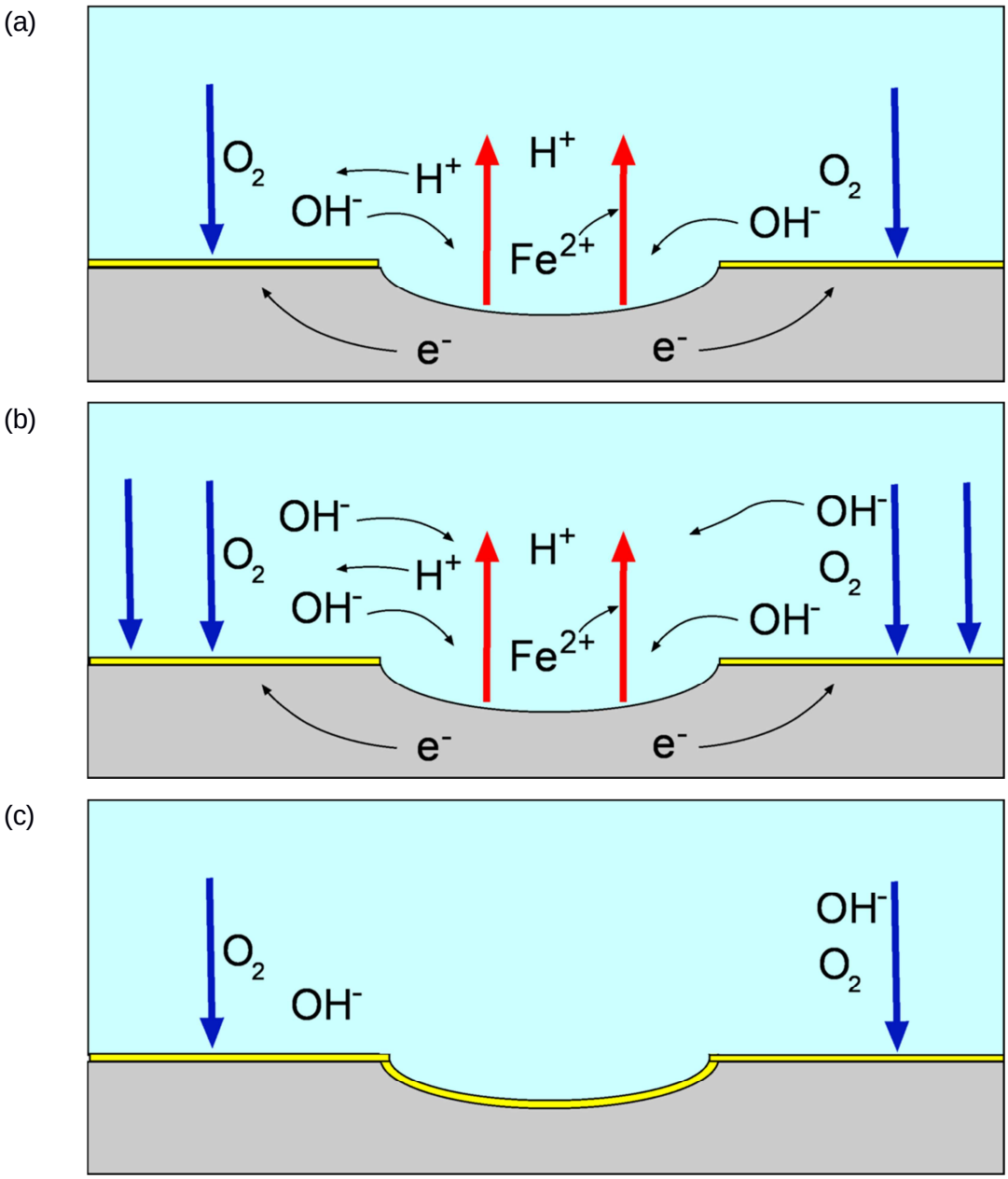

Figure 11: **Galvanic corrosion between a passive steel cathode and a local anode: a) No external cathodic current; b) Cathodic protection resulting in a net pH increase in the electrolyte; c) Passivation of the anode under cathodic protection.**

While the local corrosion process in a partially passivated coating defect can result in relevant corrosion rates of up to 6mm/year, an increasing protection current density will cause an important pH increase in the soil adjacent to the coating defect due to the concentration polarization. Since the anodic current on the active site will cause migration of negatively charged ions to the anode, a continuous transport of hydroxides to the anode will establish. If the pH is sufficiently increased and no relevant concentration of other anions such as sulfates and chlorides are present, the decrease of the pH in the anode should be hindered. If additional to migration, relevant diffusion of hydroxide to the anode is taking place, an increase of the pH in the anode and subsequent passivation can be expected. This passivation is further supported by the increased Fe^{2+} concentration expected to be present at the anode. Based on this consideration migration and diffusion of hydroxide could be the controlling process that may allow for complete passivation of the steel surface. This mechanism is schematically illustrated Figure 11. In the case of galvanic corrosion the hydroxide ions generated at the cathode are

sufficient to provide passivity. However, it may not provide a relevant increase of the pH in the electrolyte in the vicinity of the anode to compensate for its acidification (Figure 11a). In presence of a net cathodic current entering the steel surface in the case of a cathodic protection, the concentration of hydroxide ions is increased at the cathode. From the stoichiometric point of view this allows for neutralization of the acidification at the anode and further increase of the pH as shown in Figure 11b. The transport of the hydroxides is achieved through migration caused by the galvanic current and diffusion due to the increased concentration gradient. The combined migration and diffusion is expected to sufficiently increase the pH at the steel surface and provide passivation of the former anode according to Figure 11c. From the point of view of the corrosion mechanism it is not relevant whether the increase in pH is achieved through a general alkalinity as present in concrete or by a net increase of the pH in a near neutral soil within the vicinity of a coating defect as a result of the cathodic current.

4. Conclusions

Based on the literature results obtained in field tests [8, 10] locally increased corrosion rates can be obtained even when the protection criteria of ISO 15589-1 are met. The presented laboratory investigations as well as numerical considerations indicate that this increased local corrosion rates can be readily explained based partial passivation and the resulting heterogeneous current distribution within individual coating defects. The presented results indicate that the local corrosion rate may increase under the following circumstances:

- Increasing coating defect size
- Increasing aeration of the soil
- Increasing soil resistivity

Despite of limited mass transport conditions and increased pH at the steel surface this corrosion cannot be assessed and excluded, neither with a sufficiently negative on-potential nor an IR-free potential measurement, as shown in Figure 1.

While substantial corrosion rates well above 0.1 mm/year can be expected, there is reason to believe that the corrosion rate could decrease over time. This is a result of the increase of the pH at the cathodic surface, the accumulation of Fe^{2+} at the anode as well as combined migration and diffusion of hydroxide ions. While within the performed experiments it was possible to confirm that a general repassivation can take place, it is not possible to exclude continued corrosion under specifically adverse configurations. This is true for extreme cases of the items listed above and all instances where the increase of the pH is limited due to acidic soil, high levels of carbonates, a high buffer capacity of the soil solution as well as streaming water.

Based on these results the application of on-potential values significantly more negative than -1.2 V_{CSE} is expected to decrease the risk of heterogeneous passivation. This is in line with most recent statistical evaluation of pigging and on-potential data [17]. These data not only showed a decrease in relevant corrosion, but also increased corrosion in high resistive sandy soil.

In the light of the presented results it is crucial to install a temporary CP already during construction to prevent the formation of aeration cells from the very beginning. The DCVG at strongly increased rectifier output, which is often used as a quality control after commissioning, will contribute to the passivation of the remaining local anodes. Therefore, a repetitive temporary shift of the on-potential to more negative values can provide beneficial effects for the durability

of the pipeline and the effectiveness of CP. In this context, however, it is important to consider the relevant effects on ac-corrosion as described in ISO 18086 and the corresponding literature [18].

5. Literature

1. R. J. Kuhn, "Galvanic current on cast iron pipes", *Bureau of Standards, Washington, Soil Corrosion Conference*, 73 (1928).
2. K. Kasahara, T. Sato, H. Adachi, "Results of Polarization Potential and Current Density Surveys on Existing Buried Pipelines", *Materials Performance* **19**, 49 (1980).
3. N. G. Thompson, T. J. Barlo, "Fundamental process of cathodically protecting steel pipelines", in Gas Research Conference, Government Institute, Rockville, MD, USA, (1983).
4. M. Pourbaix, "Atlas of electrochemical equilibria in aqueous solutions". (NACE, Houston, TX, 1974).
5. U. Angst *et al.*, "Cathodic protection of soil buried steel pipelines – a critical discussion of protection criteria and threshold values", *Materials and Corrosion* **11**, 9 (2016).
6. L. I. Freiman, I. V. Strizhevskii, M. Y. Yunovich, "Passivation of iron in soil with cathodic protection", *Protection of Metals* **24**, 104 (1988).
7. M. Büchler, "A New Perspective on Cathodic Protection Criteria Promotes Discussion", *Materials Performance* **54, No 1**, 44 (2015).
8. D. Funk, H. Hildebrand, W. Prinz, W. Schwenk, "Korrosion und kathodischer Korrosionsschutz von unlegiertem Stahl in Sandböden", *Werkstoffe und Korrosion* **38**, 719 (1987).
9. U. R. Evans, "The electrochemical character of corrosion", in Annual Autumm Meeting, Manchester, p. 239 297, (1923).
10. T. J. Barlo, "Field Testing the Criteria for Cathodic Protection of buried Pipelines". PRCI, Ed., PRCI (Technical Toolboxes, Inc. Housten Texas, Houston, 1994).
11. M. Büchler, "Physical-chemical significance of the IR-free potential and methods for assessing the effectiveness of cathodic protection", *3R special* **Special 01/2014**, 42 (2014).
12. M. Büchler, "Über die physikalisch-chemische Bedeutung des IR-freien Potentials und alternative Verfahren zum Nachweis der Wirksamkeit des kathodischen Korrosionsschutzes", *3R* **06/2014**, 8 (2014).
13. M. Büchler, "Schutzkriterien für den kathodischen Korrosionsschutz", *Aqua & Gas* **94**, 12 (2014).
14. W. v. Baeckmann, W. Schwenk, W. Prinz, "Handbuch des kathodischen Korrosionsschutzes Theorie und Praxis der elektrochemischen Schutzverfahren". (VCH Verlagsgesellschaft Weinheim, 1989).
15. M. Büchler, D. Joos, "Die Wechselstromkorrosionsgeschwindigkeit: Die relevanten Einflussgrößen sowie deren Bedeutung für die Dauerhaftigkeit

von kathodisch geschützten Rohrleitungen", *DVGW - energie/wasser-praxis*, 54 (2016).

16. M. Büchler, D. Joos, "AC-corrosion on cathodically protected pipelines: A discussion of the involved processes and their consequences on mitigation measures", in The european corrosion congress EUROCORR, Dechema e.V., (2016).
17. R. Coster, "Statistical modelling of external corrosion based on CP history ", in CEOCOR international Congress 2016 Ljubljana, CEOCOR, c/o SYNERGRID, Brussels, Belgium, (2016).
18. M. Büchler, "Alternating current corrosion of cathodically protected pipelines: Discussion of the involved processes and their consequences on the critical interference values", *Materials and Corrosion* **63**, 1181 (2012).